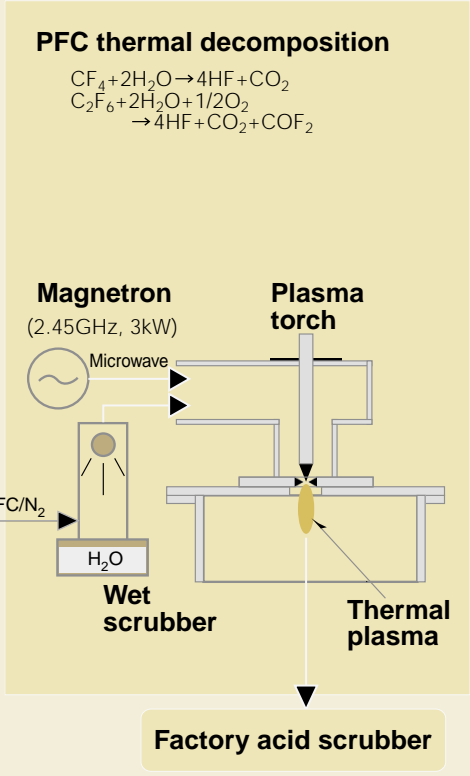
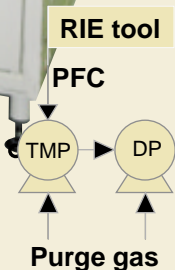


MITSUBISHI ELECTRIC ADVANCE

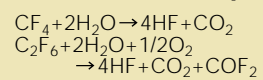
Environmental Technology Edition



TMP : Turbo molecular pump
DP : Dry pump
RIE : Reactive Ion etching



PFC thermal decomposition



Magnetron
(2.45GHz, 3kW)

Plasma torch

Wet scrubber

Thermal plasma

Factory acid scrubber

Environmental Technology Edition

CONTENTS

TECHNICAL REPORTS

Overview	1
<i>by Susumu Hoshinouchi</i>	
Trial Calculation of the Eco-Efficiency Indicator for Electrical Appliances	2
<i>by Tetsuya Takahashi and Kiyoshi Ueno</i>	
New Production Technology Building Meets Energy Saving Challenge	6
<i>by Tomofusa Uchiyama</i>	

R&D PROGRESS REPORTS

Recycling of Polyurethane Foam Refrigerator Insulation	10
<i>by Michio Murai and Tsukasa Takagi</i>	
A Thermosetting/Thermoplastic Hybrid for Easy Decomposition	13
<i>by Hiromi Ito and Kenji Mimura</i>	
Recovering Phosphates from Sewage Sludge	17
<i>by Nozomu Yasunaga and Junji Hirotsuji</i>	
Clean Combustion for Use in Indoor Environments	21
<i>by Minoru Sato and Hiroaki Shigeoka</i>	
Plasma PFC Abatement at Atmospheric Pressure	24
<i>by Yasutaka Inanaga and Kiyohiko Yoshida</i>	

Cover Story

Our cover story for this special issue shows equipment for decomposing perfluoro compounds (PFCs), with their extremely high global-warming potential, associated with reactive ion etching (RIE) tools. It can handle the PFC abatement requirements of gas vented from RIE chambers at a flow rate of 30slm (CF₄/N₂). Because decomposition occurs at atmospheric pressure, treatment can, of course, be performed downstream of the vacuum-pump system and, taking advantage of the quick-start properties of the plasma method used, it can be readily operated only when the RIE chambers are in use, enabling energy-saving operation matched to the abatement load.

Editor-in-Chief

Kiyoshi Ide

Editorial Advisors

Chisato Kobayashi
 Koji Kuwahara
 Keizo Hama
 Katsuto Nakajima
 Hiroshi Hasegawa
 Hiroshi Muramatsu
 Noriichi Tajima
 Fuminobu Hidani
 Yukio Kurohata
 Hiroshi Yamaki
 Kiyohide Tsutsumi
 Osamu Matsumoto
 Hiromasa Nakagawa

Vol. 104 Feature Articles Editor

Hiromu Narumiya

Editorial Inquiries

Keizo Hama
 Corporate Total Productivity Management
 & Environmental Programs
 Fax 03-3218-2465

Product Inquiries

Hiromu Narumiya
 Corporate Environmental Sustainability Group
 Corporate Total Productivity
 Management & Environmental Programs
 Mitsubishi Electric Corporation
 2-2-3 Marunouchi
 Chiyoda-ku, Tokyo 100-8310, Japan

Mitsubishi Electric Advance is published on line quarterly (in March, June, September, and December) by Mitsubishi Electric Corporation.

Copyright © 2003 by Mitsubishi Electric Corporation; all rights reserved.
 Printed in Japan.

Overview

Taking up the Challenge of Engineering for Recycling



*by Susumu Hoshinouchi**

The formation of a sustainable economy based on recycling is one of the most urgent necessities facing Japan in the 21st century.

As indicated by the Ministry of Economy, Trade and Industry's Industrial Structure Council, establishing a specific body of engineering expertise in recycling as a new sector of industrial technology and an ongoing succession of separate, specific reforms are indispensable to form a sustainable economy based on recycling and to integrate the environment into the economy. This body of expertise in recycling will have both to reduce the environmental burden imposed by products throughout their entire life cycles and to reduce the energy resources needed to recycle them.

Mitsubishi Electric Corporation takes the initial letters of three prime concerns, those over the materials used (M), the energy required (E), and the toxicity of the wastes generated (T), and uses the acronym MET to express its commitment to an integrated approach to solving the technological problems. This approach addresses both problems associated directly with the product and those concerning the manufacturing processes that create it. The result of this two-fold approach has been the development of innovative proprietary environmental technologies that are not only economically viable but also highly competitive in the market place.

The United Nations' World Commission on Environment and Development issued a report entitled "Our Common Future" in which the environment and development are both recognized as vitally important for the future of mankind. With a renewed awareness of this fact, Mitsubishi Electric is taking up the challenge of creating technology upon which a sustainable society can be based. □

**Dr. Susumu Hoshinouchi is General Manager, Corporate Environmental Sustainability Group.*

Trial Calculation of the Eco-Efficiency Indicator for Electrical Appliances

By Tetsuya Takahashi and Kiyoshi Ueno*

To realize a sustainable society it is necessary to ensure that economic growth can be made comparable with the reduction of material consumption. Improvement of eco-efficiency has thus become an issue. To focus attention on the eco-efficiency of products in a concrete way, Mitsubishi Electric has applied Factor X. In December 2001, to solicit feedback that would help refine the formula, the corporation made public the evaluation method for this factor and the results of calculating it for some of its products. This article summarizes this procedure, its results, and subsequent developments.

What is Factor X, the Product Eco-Efficiency Indicator?

BASIC CONCEPT AND CHARACTERISTICS. The idea of such a factor has been advocated in Europe and America. It arose from the concern to ensure a sustainable society by reducing raw material resource requirements while at the same time raising the amount of economic value added and improving the convenience of daily life. One original proposal was 'Factor 4,' developed by Dr. Ernst von Weizsacher, former head of the Wuppertal Institute. This was intended to indicate the need to reduce to one quarter the amount of energy resources required by advanced countries and improve the resource efficiency and eco-efficiency by a factor of four.

Another proposal was 'Factor X' formulated by Professor Ryoichi Yamamoto's group at The University of Tokyo. In deriving values for this factor, neither the target year for implementation nor the methods of quantification were specified. Our factor uses the formula below, which is based on the above-mentioned concepts, where eco-efficiency (EE) = product performance (P) divided by negative environmental impact (I).

$$\begin{aligned} \text{Thus, Factor X} &= \Delta EE \\ &= EE_{\text{new}}/EE_{\text{old}} \\ &= (P_{\text{new}}/I_{\text{new}})/(P_{\text{old}}/I_{\text{old}}), \\ &= \frac{\text{Performance Improvement}}{\text{Environmental Impact Reduction}} \end{aligned}$$

or, in words, the factor by which the eco-effi-

ciency of the new product exceeds that of the old product divided by the factor by which the negative environmental impact has been reduced. Here;

EE_{new} : new product eco-efficiency,

EE_{old} : old product eco-efficiency,

P_{new} : new product performance,

I_{new} : new product negative environmental impact,

P_{old} : old product performance, and

I_{old} : old product negative environmental impact.

It therefore follows that for a negative environmental impact 1/Xth lower than before, with unchanged product performance and service, the eco-efficiency would increase X-fold (Factor X). Unlike life-cycle assessment (LCA), the factor does not only indicate the degree of reduced negative environmental impact but is also able to reflect product performance and service improvements.

General Factors of Computation

The numerator of the factor is the degree of performance improvement. If a product's performance shows remarkable improvement, even if the degree of reduction of negative environmental impact of the product is low, the resultant factor value rises in appearance only; the extent of the contribution made by reducing negative environmental impact is unclear.

If novel functions that were not provided by previous products are added, the numerator becomes indefinitely large. Moreover, if the use of substances that are potentially harmful to the environment is completely eliminated, such as implementation of lead-free measures, the denominator (degree of improvement of negative environmental impact) becomes zero and the factor value becomes indefinitely large. This poses problems for the meaningful quantification of the denominator and numerator.

Usually, the numerator, which represents the degree of improvement in performance, is not a single factor but a number of different factors. The denominator, which contributes to the improvement of negative environmental impact is also a factor. At issue is the method of integrating these independent factors.

By weighting each of the components for prod-

*Tetsuya Takahashi is with the Corporate Environmental Sustainability Group and Kiyoshi Ueno is with the Living Environment and Digital Media Equipment Group.

uct performance and negative environmental impact, the means of integration can also be refined. This process both introduces subjectivity and, through the weighting procedure, consequently yields a virtual result.

Proposal for Evaluating Degree of Improvement with MET* and Vector Synthesis

Mitsubishi Electric has worked out a vector synthesis method to quantify negative environmental impact by assessing the degree of improvement of MET, and this method has been employed to calculate factor values. In this method, even if one of the MET values is zero, it is still possible to quantify by using a vector sum. If improvements are not balanced, the numerical value is limited and the factor value does not rise. There are some products, such as certain household electrical appliances and heavy electrical equipment, that are unlikely to undergo any remarkable revolutionary advances in technology. Because it is difficult to evaluate this type using only a factor value, their 'level of social contribution through reduction of the negative environmental impact of the product' is also assessed.

*MET should be understood as follows:
M, material (effective utilization of resources);
E, energy (effective utilization of energy);
T, toxicity (avoidance of use of substances that are potentially harmful to the environment).

Basic Concept in Calculating the Eco-Efficiency Indicator 'Factor'

In principle, products in the 1990 fiscal year are defined as standard products and they are compared with present products.

FACTOR NUMERATORS. If no improvement can clearly be evaluated between old and new products with regard to performance, function, service, or quality, the value is taken as 1.

FACTOR DENOMINATOR. MET, which symbolizes the basic approach to reducing negative environmental impact in the Mitsubishi Electric Group, was used for evaluation. To evaluate the product's contribution to the reduction of negative environmental impact in terms of MET, the calculation of the environmental impact of each of the MET components is, as far

as possible, simplified and combined. That is, if the three components,

1. Amount of negative environmental impact during use of resources (*M*),*
 2. Amount of energy used (*E*), and
 3. Amount of substances that are potentially harmful to the environment used (*T*),
- are, for standard products, given a value of 1 when included in calculations of the negative

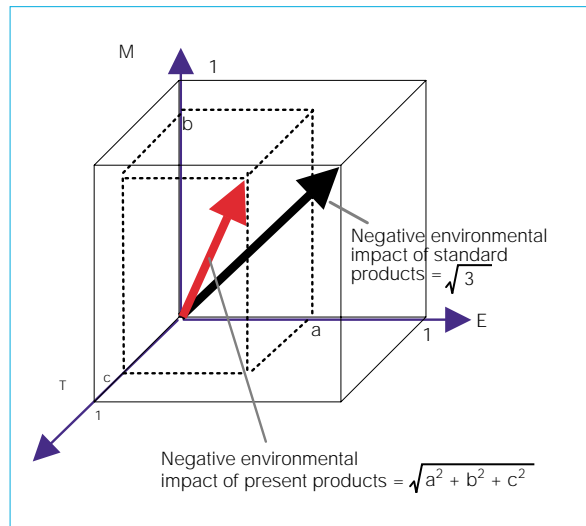


Fig. 1 Application of vector synthesis to evaluate negative environmental impact.

environmental impact (*a*, *b*, *c*) of standard products, they are combined as vector lengths (see Fig. 1).

The actual formula is as follows:
 Factor = eco-efficiency of present product (*A*) divided by eco-efficiency of standard product (*B*), where

$$A = 1/\sqrt{(a^2 + b^2 + c^2)}$$

$$B = 1/\sqrt{(1^2 + 1^2 + 1^2)} = 1/\sqrt{3}$$

The negative environmental impact of the effective utilization of resources (*M*) is derived from the expression given below:

Amount of negative environmental impact of effective utilization resources
 = amount of consumption of virgin resources (*M*₁) + amount of materials that are not recycled and have to be disposed of at end of product life (*M*₂)

$$= [\text{product mass} - \text{mass of recycled materials and recycled parts}] + [\text{product mass} - \text{mass of recyclable materials}]$$

BOUNDARY LIMITS. In principle, the material boundary is considered to be the entire life cycle of a product from the time the original raw material is extracted to the end of the product's life.

CALCULATION OF DEGREE OF SOCIAL CONTRIBUTION TO ENVIRONMENT. Although this is different from the 'Factor,' the conditions of calculation are the same as above. On a per-unit basis, the reduction in the amount of virgin materials used, the reduction in the amount of electricity consumed multiplied by hours of use over the product lifetime, and reduction in the usage amount of substances that are potentially harmful to the environment are evaluated. Each of these values are multiplied by the total sales (number of units) of the item in question during the preceding annual period.

Practical Application

Table 1 shows the results of factor trial calculations for some of the company products. These and applied results for some other products are disclosed in the Mitsubishi Electric Group's 2003 Sustainability Report, available at the following URL.
<http://www.MitsubishiElectric.co.jp/corporate/eco/>

Factor Indicator: Issues and Future Prospects

LEVEL OF AWARENESS OF INDICATORS. The definition of the factor, standard product, and calculation method, are all different depending on the enterprise. Since the factor is an in-house relative indicator that is employed to show the level of improvement between current and former products made by the same company, the value of this factor must not be compared with the value of factors published by other companies. Outside of the company, consumers are insufficiently aware of the existence of the factor and how it is defined. It needs to be explained and understood that factor formulas are not worked out for the convenience or advantage of the company. Effort is needed to raise its value in the market.

INCENTIVE TO PRODUCT DESIGNERS. Unlike LCA, the bigger the Factor value, the better it is. This makes it a legitimate tool for evaluating ability against the expertise of designers of preceding products. As an 'indicator of bright prospects for the future,' it also gives incentive to product designers.

EVALUATION OF DEGREE OF IMPROVEMENT OF PRODUCT FUNCTIONS AND SERVICE. The Japanese Ministry of Economy, Trade and Industry is studying how to bring about standardization of methods to quantify the degree of improvement of product functions and reduction of nega-

Table 1 Values Resulting from Application of Factor Calculation to Some Mitsubishi Electric Products.

Products	Models Compared		Environmental Impact			Factor	Contribution to Society
	Former	New Product	MET	Former	New Product		
Air conditioners	MSZ2800 (1990)	MSZ-WX28J (2002)	M E T	1 1 1	0.96 0.48 0.54	1.44	400 tons less materials 1,870GWh less energy 0.8 tons less lead
Refrigerators	MR-C36H (1993)	MR-Y40B (2002)	M E T	1 1 1	0.95 0.6 0.0	1.54	176 tons less materials 176GWh less energy Scheduled fluorocarbons eliminated (70.4 tons)
Automatic washing machines	AW-80V1 (1991)	MAW-V8TP (2002)	M E T	1 1 1	0.59 0.37 0.51	2.0	5,700 tons less materials, 230m liters less water. 90GWh less energy 3 tons less lead
Color TVs	25C-X30 (1996)	25T-D101S (2002)	M E T	1 1 1	0.93 0.64 0.67	1.33	Polystyrene foam eliminated (3.16 tons) 31.6GWh less energy 0.04 tons less lead, 12.3 tons less chlorinated flame retardants.

tive environmental impact, development of factor indicators, and other evaluative techniques. Close examination of these techniques will enable performance evaluation indicators to be properly verified. To enable the adoption of verifiable indicators, the definition and method of calculation of the original factor will be revised.

If it were possible to quantify the forces that drive the creation of eco-products, improvement of performance and reduction in negative environmental impact, they could be harnessed to become the driving force behind genuine 'Eco-products.' Moreover, to meet the ISO140001 stipulation of continuous improvement, the only way is to work to improve products so that the factor values for eco-efficiency rise every year.

REQUESTS FROM CUSTOMERS FOR ENVIRONMENTAL INFORMATION ABOUT PRODUCTS. When making factor values known, to avoid the risks of "going it alone" in revealing values, it is also necessary to be prepared to disclose the product models used for comparison, calculation techniques, indicators, weighting, method of combination, and other aspects. Since the calculations are made comparing the company's current and former models, it is also necessary to let it be known that the data cannot be compared with the data for products made by other companies.

In Mitsubishi Electric's Fourth Environmental Plan (dated February 2003), improvement of eco-efficiency to ensure reduced negative environmental impact throughout the life cycle of the product is targeted for the creation of Eco-products and Hybrid Eco-products. To realize a sustainable society, for the time being, we have to aim to meet the challenges set by Factor 4. With the indicators that we have conceived and the proposed calculation methods to establish the values, we hope to contribute to global standardization. On the occasion of the introduction of Factor X within our corporate group, we take the opportunity to make special mention of the debt of gratitude that we owe to Professor Ryoichi Yamamoto, of The University of Tokyo Center for Collaborative Research, for his guidance and advice. □

New Production Technology Building Meets Energy Saving Challenge

by Tomofusa Uchiyama*

At the site of Mitsubishi Electric's Communication Systems Center, to provide space for technical development and trial production, the corporation has built the new production technology building shown in Fig. 1. During the basic architectural planning stage, on the principle of building an environmentally friendly facility, priority was given to using natural energy. Moreover, centered on the corporation's low-energy products, the construction gave us a chance to apply energy-saving technologies and ideas aggressively. The building succeeded in further reducing environmental impact, especially by minimizing the effects of energy use on the environment.

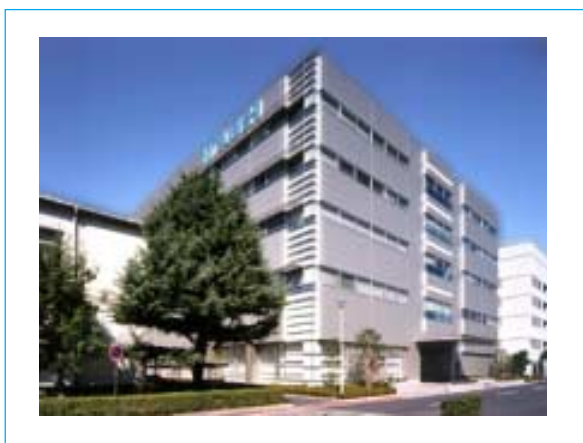


Fig. 1 The newly built production technology building

Central Concept: Energy Saving

The building was designed to test the effective promotion of reduced consumption of energy by practically implementing the use of natural energy, eradicating energy waste through optimized control, and energy-saving through monitoring and automation. Moreover, by favoring Mitsubishi Electric equipment for the installation, we were able to take full advantage of our own power-saving devices.

Building-Design Features

The basic floor plan extended 40m north to south and 90m east to west. From this footprint it was necessary to secure maximum layout flexibility for room spaces in 90m by 15m north-south strips.

Consequently, an optimized core design was adopted. The challenge then became to illuminate the central areas, which were distant from outer walls, and to implement natural ventilation. To maintain the core arrangement on a north-south axis, two ventilation machine rooms and outgoing airshafts were located at two places in the central area as shown in Fig. 2.

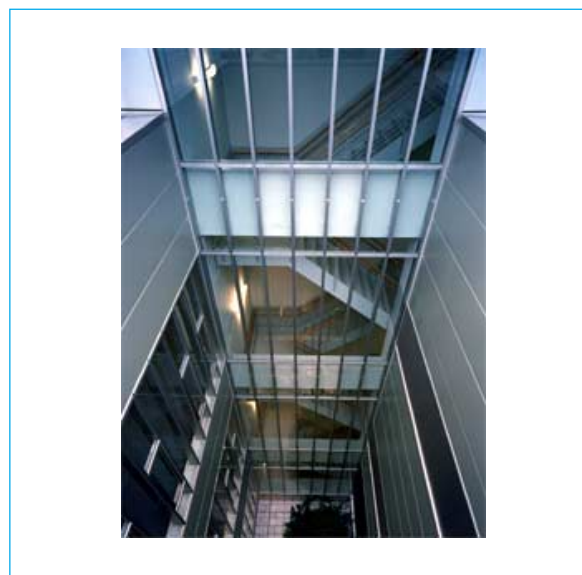


Fig. 2 Out airshaft locations

Room space and stairwells surrounding the out airshafts were walled with glass to let in light so that the stairways, even though they are at the center of the building, could be naturally lit, see Fig. 3. Moreover, the ventilation machine rooms, located at the stairwells, are able to take in air even though they are situated at the center of the building.

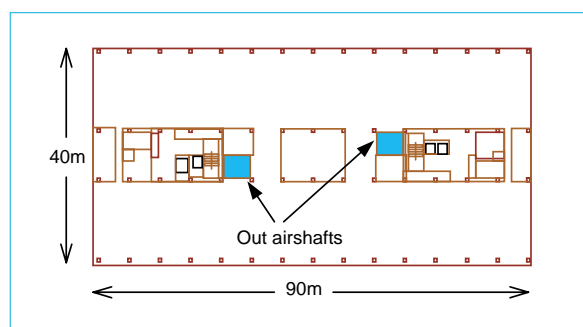


Fig. 3 Out airshaft

*Tomofusa Uchiyama is with the Communication Systems Center.

Meanwhile, the long south-facing frontage lets sunlight directly into the room space through the windows. There was concern that this would increase the air-conditioning load during the summer, so aluminum louvers were fitted above the windows to block direct sunlight and cut the cooling load.

Adiabatic Performance of the Building

If the material used for the outer wall of a structure has a low overall heat-transfer coefficient, it can greatly improve the adiabatic performance. High-insulation sheet-steel sandwich panels were used. The overall heat-transfer coefficient of these high-insulation sheet-steel sandwich panels was 65% less than the extruded cement panels that have hitherto been used. Excellent adiabatic performance can be expected. Although ALC (autoclaved lightweight concrete) has about the same overall heat-transfer coefficient as high-insulation sheet-steel sandwich panels, it requires regular coating treatment, which leads to greater environmental impact over the long term. The final choice reflected this, along with styling and other design considerations.

The roof structure was designed to allow for future roof greening, which will prevent the penetration of radiant heat. It was finished with lightweight concrete and, to improve the insulation properties, double the usual thickness of polystyrene insulation.

Air-Conditioning System

Because the design, testing, and other departments are going to share the structural space for rooms, it has been designed for frequent re-

arrangement and alteration. The activities of different departments mean that hours of operation (working hours) and cooling load (area) will also be subject to great variability. Consequently, equipment was installed to provide local fine control and response to load variations. Multi-unit air conditioning, comprising distributed units and an air-cooled heat-pump system with superior thermal efficiency, was therefore used.

Furthermore, to reduce peak loading during the summer, ice-storage air-conditioning units were installed in clusters at places that would receive the greatest thermal loading from sunlight. Non-ice thermal-storage air-conditioning equipment was used for production areas operating around the clock and for the central indoor area with little thermal loading from sunlight, achieving an optimal arrangement of the equipment. As a result, 60% of the cooling capacity is provided by ice thermal storage and a 22% reduction in peak demand has been achieved.

Outside Air Cooling

In mid season, when the outside air temperature is low, to reduce the need for air-conditioner operation, an active effort was made to use the external air to cool the interior space. This system comes into operation depending on the interior and exterior temperatures. To ensure that a proper interior temperature is maintained after the system cuts in, inverters are installed to automatically regulate the inflow of air.

Ventilation System

To minimize loading from cooling, heat is recovered from outgoing air by an energy-recovery ventilator system (using proprietary "Lossnay" products).

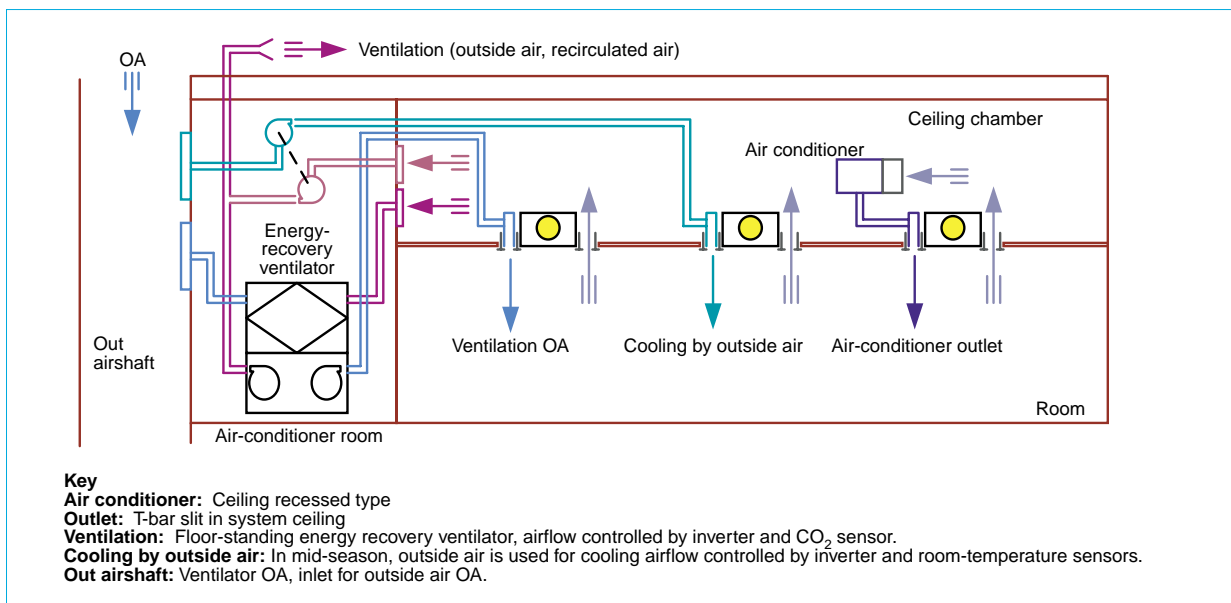


Fig. 4 Configuration of air-conditioning system

Furthermore, to regulate ventilation, the level of carbon dioxide is monitored. To maintain values below a set level, an inverter automatically controls the amount of ventilation. Thus, the system minimizes both heat wastage and the energy consumed by operating the ventilation system.

Fig. 4 schematically shows the air conditioning, external air cooling, and ventilation system.

Lighting System

For lighting, the building has an automatically adjusting system comprising high-efficiency HF-inverter fluorescent-lighting fixtures with continuous autodimming. The level of illumination provided by the fixtures depends on sensors that monitor zones near the windows, the interior side of the room, and the core areas. In this way, power economy is achieved by automatically adjusting light, especially in the naturally illuminated areas near windows. Compared with the ordinary systems that have been commonly used up to now, the new system consumes 43% less power.

In rest rooms, stairwells, corridors, and other shared spaces, to achieve power economy, lights are automatically turned on and off by human-movement sensors.

Power Substation Equipment

Power losses (both no-load loss and load loss)

have been minimized by using an ultrahigh efficiency high-current transformer. Compared with previous equipment the power loss has been cut by 23%.

Use of New Energy

Photovoltaic cells that generate 10kW of electrical power have been installed on the roof. These interconnect with the rooftop electrical installation and the solar-generated current power devices inside the structure without wastage.

Central Monitoring System

A MELBAS-AD, linked to the subsystems, is installed at the core of the central monitoring system. The subsystems comprise B/Net for the illumination, power panels, and power metering, MELANS (MJ-300) for integrated monitoring of the air-conditioning system, and MELSAFETY for security monitoring, as shown in Fig. 5.

Control Schedule

So that room occupants can carry out basic control, local operation switches are provided in each area to enable on and off switching of illumination and air conditioning. During rest periods, at night, and at other periods of non-occupancy, however, at fixed times the services are switched off according to a preset schedule. This minimizes power wastage when people forget to switch off lights and other equipment.

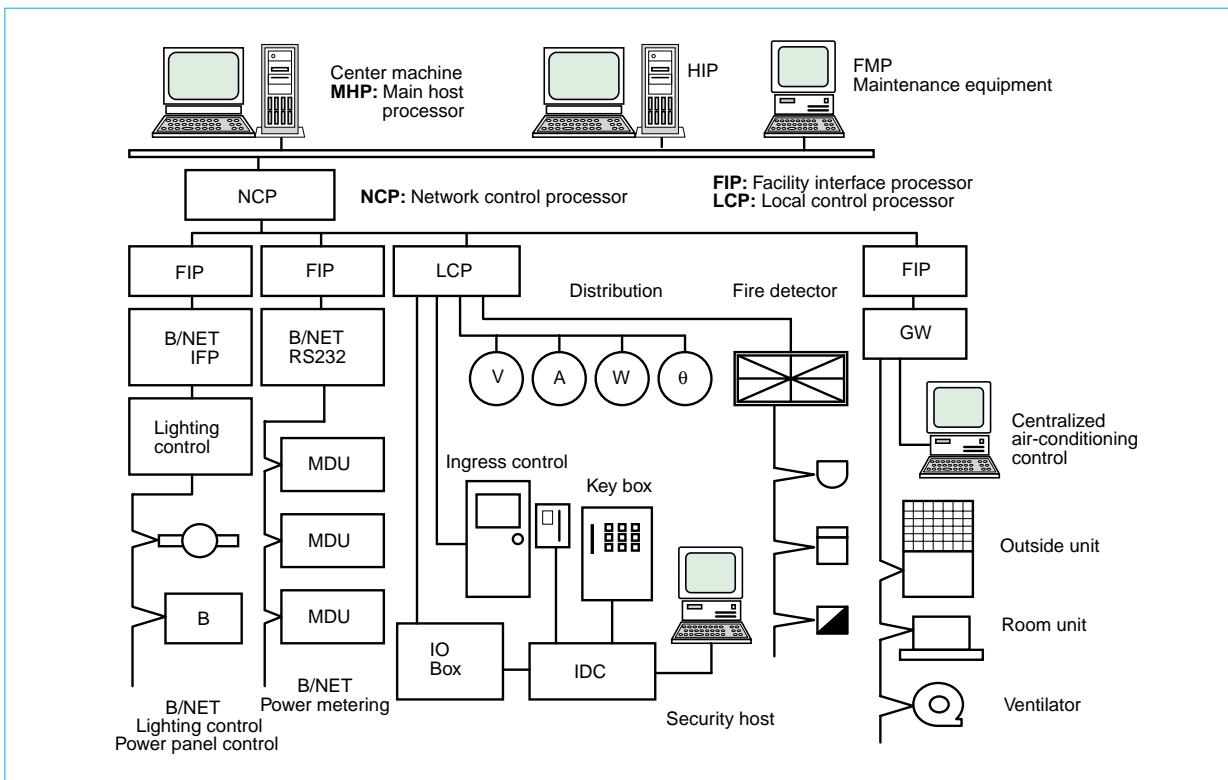


Fig. 5 Configuration of building monitoring system.

Table 1 List of Mitsubishi Electric Equipment Installed in the New Building.

The energy-saving Mitsubishi Electric equipment used		Type/Name
Air conditioners	Multi-unit heat-pump type air conditioners with heat storage	City Multi ICE-Y
Ventilators	Stationary-type energy-recovery ventilators	Lossnay
Distribution equipment	Highly efficient transformers	RA-T
	No-Fuse circuit breakers (with instrument displays)	MDU
	Solar energy electrical generator	PV-MG007F
Lighting equipment	High-frequency continuously variable inverter-type fluorescent lights	Fine Base
	Automatic lighting control using natural light	MELSAVE
Control equipment	Inverters	FREQROL-A Series
Monitoring equipment	Central monitoring and control equipment for the entire building	MELBAS-AD
	Centralized air-conditioning monitoring and control equipment	MELANS (MJ-300)
	Security monitoring and control equipment	MELSAFETY-S10
Elevators	VVVF inverter-controlled elevators	GRANDEE

Operation Management Geared to Security

As each floor is locked, power supply to all but continuously operating equipment is shut down at the power panel, and air conditioning, ventilation, and lighting are automatically switched off. This cuts standby mains power consumption and reduces wastage if occupants forget to turn off lights, air conditioning, and other services.

Peak-Power Reduction Control

To reduce consumption at peak power, on receipt of peak-power signals, in a preset order, the air conditioning central monitoring equipment overrides other controls and resets units to blow-only mode.

Control of Power Metering

The main breaker of each power panel is fitted with an MDU (measuring display unit). Meanwhile, the current is centrally monitored by B/Net. At present, the meters of all the structures on site are connected and the data is used for energy-saving activities.

The energy-saving measures that were implemented have saved 22% more energy than if previous methods had been used. Although simple performance improvements account for some of the reduction, other measures were unproven at the design stage and required practical investigation. Moreover, because of the general-purpose nature of the building, it is likely to be used for a considerable length of time. To prevent energy loss that would continue throughout the entire life of the building, it was essential to consider energy saving. Given delivery, budgetary, and other constraints at the planning stage, it is important to evaluate how effective the adoption of these measures has

been. Table 1 is a final list of the Mitsubishi energy-saving equipment that was installed in the building. We will continue to apply our ingenuity to create ideal energy-saving building designs and, as part of our contribution to environmental improvement, also promote energy conservation by improving the performance of existing buildings. □

Recycling of Polyurethane Foam Refrigerator Insulation

by Michio Murai and Tsukasa Takagi

A degradation solvent was developed for glycolysis of the polyurethane foam used in refrigerator thermal insulation. With this solvent, recycled polyols were quickly obtained that had performance similar to virgin materials. Moreover, refrigerator thermal insulation made from this recycle had performance similar to that of virgin materials.

Chemical Recycling of Polyurethane

Chemical recycling is one of the methods of recycling waste polyurethane foam (PUF). Glycolysis, hydrolysis, aminolysis and other chemical processes for degrading PUF into low molecular weight compounds are widely known.^{[1],[2]} In glycolysis, PUF is converted to low molecular weight polyols by transesterification. Up to now, however, the reuse of polyols recovered from chemical recycling has yielded polyurethane resins with performance that is inferior to virgin materials. This, and other disadvantages such as the low efficiency of degrading the voluminous foamed products that are usually made from polyurethane resins, has meant that chemical recycling finds little practical use. At Mitsubishi Electric, using glycol dissolution, we have carried out the degradation of waste refrigerator insulation PUF into polyols in short processing periods. This process has been developed into reuse technology that processes waste PUF as a raw material. Here we present a brief discussion of this technology.

Solubility of PUF

To examine the dissolution time for PUF in various glycolysis conditions, we adopted a simple experimental procedure. After the solution was heated to a temperature of 170°C~200°C, a 3cm cube of rigid PUF was completely immersed in a glycol solution of catalyst. The time from immersing the PUF to its complete disappearance

was recorded as the PUF dissolution time.

Table 1 shows PUF dissolution times in various glycol and amine solutions of KOH (potassium hydroxide). DEA (diethanolamine) dissolved PUF in the shortest time. This is because the secondary amine group on the DEA molecule promotes the cleavage of the urethane bond.^[3] PUF dissolution time depends on the molecular weight of glycol. DPG (dipropylene glycol) dissolves PUF in the shortest time. Similarly, we examined PUF dissolution times in high functionality polyols derived from sucrose, sorbitol, and tolylenediamine, which are commonly used as raw materials for PUF thermal insulation.^[4] These polyols take longer to dissolve PUF than glycols. Table 2 shows PUF dissolution times in DPG solu-

Table 1 PUF Dissolution Time with Various Glycol Solutions of KOH (conc. 0.2wt% at 180°C)

Glycol	Molecular weight	Dissolution time (m)
PEG		
Ethylene glycol	62	65
Diethylene glycol	106	45
Trethylene glycol	150	40
Tetraethylene glycol	194	29
Polyethylene glycol	300	52
Polyethylene glycol	400	134
PPG		
1,2-propylene glycol	76	45
Dipropylene glycol	134	19
Tripropylene glycol	192	41
Polypropylene glycol	400	136
Amine		
Triethanolamine	149	102
Diethanolamine	105	10

tions of various catalysts in equal concentrations. The solutions of alkaline metal hydroxides such as KOH and sodium hydroxide dissolve PUF more effectively than the solutions of other catalysts. Table 3 shows the influence of the KOH concentration on PUF dissolution time in DPG solutions at 180°C. PUF dissolution time is inversely proportional to KOH concentration. Fig. 1 shows the correlation between the logarithm of the PUF dissolution time $\ln(t)$ and the reciprocal of glycolysis temperature $1/T$. The straight line in Fig. 1 suggests that the glycolysis of PUF follows Arrhenius's law.

*Michio Murai is with the Advanced Technology R&D Center and Tsukasa Takagi is with Shizuoka Works.

Table 2 PUF Dissolution Time with DPG Solutions of Various Catalysts (conc. 0.2wt% at 180°C)

Catalyst	Dissolution time (m)
Sodium hydroxide	17
Potassium hydroxide	19
Sodium acetate	83
Potassium acetate	98
Dibutylindilaurate	52
Stannous octoate	165
Titanium (IV) tetrabutoxide	104
No catalyst	339

Table 3. Influence of KOH Concentration on PUF Dissolution Time in DPG Solutions at 180°C

KOH conc. (wt%)	Dissolution time (m)
0.1	40
0.2	19
0.4	10
0.6	8
0.8	5
1.0	4.5

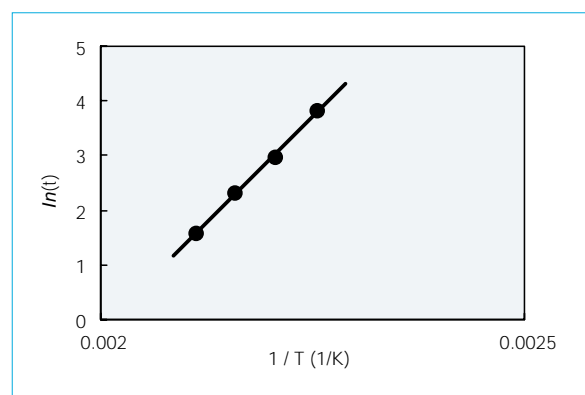


Fig. 1 Correlation between logarithm of PUF dissolution time $\ln(t)$ and reciprocal of glycolysis temperature T

Producing Recycled Polyols from PUF Glycolysis

Recycled polyols were produced in a reactor with an internal capacity of 0.2m³. A glycolysis solvent was heated to 200°C and held at that temperature for at least 15min. After the KOH dissolved in the solvent, PUF thermal insulation, cut into pieces 1cm. in diameter, was gradually added to the solvent. The solvent/PUF weight ratio was set at 1/1. Recycled polyols were obtained when four hours had elapsed from the start of feeding pieces of PUF into the solvent. In this study,

DPG, DEA, and the newly developed polyol solvent (Polyol A) were used as the glycolysis solvents. Table 4 shows the properties of the recycled polyols yielded. Those yielded by Polyol A were more viscous than other recycled polyols and had functionality and hydroxyl values that were similar to virgin polyols. In contrast, the functionality and hydroxyl values of the recycled polyols yielded by DPG and DEA were very different from the virgin polyols.

Properties of Recycled PUF Thermal Insulation Using Recycled Polyols

We used a mixture of virgin and recycled polyols to make recycled PUF thermal insulation. Isocya-

Table 4. Properties of recycled polyols

Glycolysis solvent	Polyol A	DPG	DEA
Functionality	3.5	2.4	3.5
Viscosity @25°C (mPa.s)	180000	10000	13000
Hydroxyl value (mgKH/g)	450	540	880

anate, blowing agent, catalyst, surfactant, and all other materials other than the polyols were the same virgin materials that would normally be used. Fig. 2 shows the thermal conductivity and compressive strength of PUF with recycled polyols yielded by Polyol A. In Fig. 2, the property index indicates a figure derived by dividing (property of recycled PUF) by (property of virgin PUF) multiplied by 100. The total density of each PUF sample in Fig. 2 is 51kg/m³. Fig. 2 shows that the thermal conductivity of recycled PUF is nearly equal to that of virgin PUF and the proportion of recycled polyols does not affect the thermal insulation performance of the PUF. On the other hand, the proportion of recycled polyols does have a slight effect on the compressive

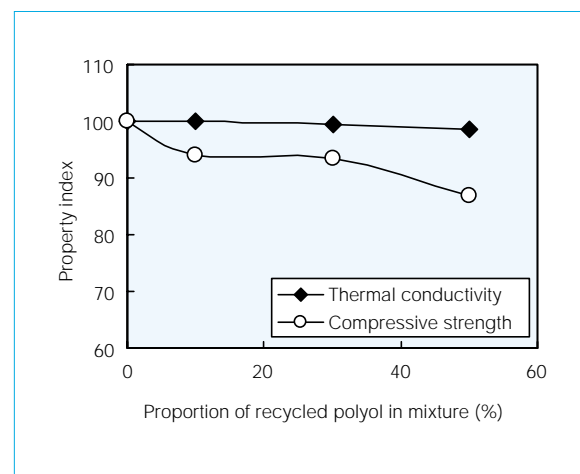


Fig. 2 Relationship between recycled polyol content and PUF properties

strength of PUF. In comparison with virgin PUF, the compressive strength of recycled PUF drops by 7% and 13% for proportions of recycled polyols of 30wt% and 50wt%.

Further, we carried out trials for the cabinets of 400L refrigerators in which we assessed the performance of recycled PUF. In these trials, we used a mixture of 30wt% of recycled polyols yielded by Polyol A and 70wt% of virgin polyols. These trials indicated that the thermal conductivity, compressive strength and dimensional stability of PUF with recycled polyols yielded by Polyol A are nearly equal to those of virgin PUF, and that this recycled PUF is suitable for use in mass producing refrigerators, despite its higher viscosity (causing the minimum fill weight of the cabinet to increase by 2%) and slightly lower adhesion.

In order to put chemical recycling of PUF to practical use for the thermal insulation of refrigerators, we will continue to improve the effectiveness of the recycling process and the quality of the recycled PUF. □

References

- [1] Oertel, G.: Polyurethane Handbook, New York: Hanser. (1993)
- [2] Wirpsza, Z.: Polyurethanes, New York: Ellis Horwood. (1993)
- [3] Kanaya, K., et al.: J. Appl. Polym. Sci., 51, 675 (1994)
- [4] Murai, M., et al.: J. Cell. Plast., 39(1), 15 (2003)

A Thermosetting/ Thermoplastic Hybrid for Easy Decomposition

by Hiromi Ito and Kenji Mimura

We have developed a hybrid of thermosetting and thermoplastic resins that improves the properties of the product during use while at the same time making it easy to decompose the resin at the end of its life cycle. The hybridization process involves blending the thermosetting resin with a small amount of thermoplastic resin, which can be broken down by organic solvents or heat. The development of a technique to reduce viscosity to improve the moldability of the blended resin remains for the future.

Introduction

Epoxy resin, phenolic resins, and other thermosetting resins possess a number of excellent characteristics including electrical insulation, desirable mechanical properties, and thermal and chemical stability. They are used in a range of electrical and electronic applications, from high-voltage electrical equipment to semiconductor devices. Once these types of thermosetting resins are cured, however, heating will not melt them and they are insoluble in most organic solvents. Consequently, at the end of the product life cycle they cause disposal problems and almost always end up in incinerators or landfills. The demand for thermosetting resins has been increasing year by year. In 1992, the Japanese market for epoxy resin, for example, was 163,000 tons. This rose to 197,000 tons in 2000. For more effective utilization of resources and to reduce the environmental impact of landfill disposal, we set out to meet the urgent need to develop a practical technology that would ease the problems of recycling.

From the point of view of materials recycling, the high proportion of filler in the thermosetting resins used for electrical and electronic devices means that components using them have little intrinsic value. Metal and other parts with some value in many electrical and electronic devices are, however, often embedded in ther-

mosetting resins. We therefore attempted to develop a thermosetting resin that would be readily decomposed so as to facilitate the recovery and reuse of these embedded parts.

Fig. 1 illustrates the development concept. Thermosetting resin, which cannot be dissolved or melted, is blended with a small amount of thermoplastic resin, which can be both broken down by solvents and melted. Then, by controlling the phase structure so that the thermoplastic resin is in continuous phase contact, the result is a thermosetting/thermoplastic hybrid. This technique, often employed to improve the heat resistance and toughness of cured resins, is known to improve the properties achieved by normal curing.^[1] To aid recovery of reusable metal parts that have intrinsic value at the end of the product life cycle, we considered a thermosetting/thermoplastic hybrid that would be readily decomposed by chemical and/or heat treatment.^[2]

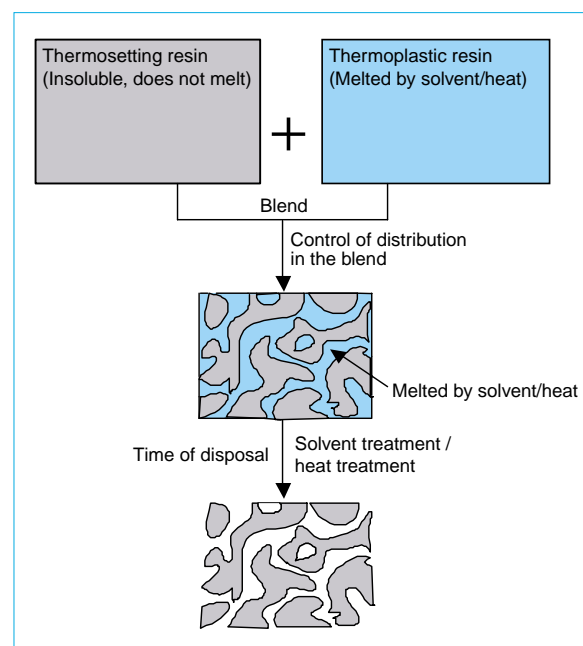


Fig. 1 The concept of a readily decomposable thermosetting resin

Readily Decomposed Resins

PHASE STRUCTURE CONTROL OF THE HYBRID. Here we report on the model resin we used to study decomposability in a hybrid that could be readily decomposed. The thermosetting resin was an epoxy type with phenolic hardener, and the thermoplastic resin was PES (polyether-sulfone). For many thermosetting/thermoplastic resin combinations, the conditions of the blend (phase), dependent on composition and tempera-

*Hiromi Ito is with the Advanced Technology R&D Center and Kenji Mimura is with Nagoya Works.

ture, result in different behaviors (phase diagrams). The thermosetting/thermoplastic blends that we used displayed a phase diagram of the LCST (lower critical solution temperature) type. If blends that display these LCST-type phase properties are formed at low temperatures, phase uniformity of the thermoplastic resin and thermosetting resin is obtained in the cured resin. If formed at high temperature, there is progressive phase separation of the thermoplastic resin from the thermosetting resin and it is reasonable to expect to obtain continuous phase with the thermoplastic resin in the cured hybrid resin.

Fig. 2 shows typical results at different formation temperatures. It is clear that varying the temperature enables control of the phase structure in the cured product. Fig. 2a shows the uniformity of the unblended cured thermosetting resin to which no thermoplastic resin had been added. Even after thermosetting resin is blended with thermoplastic resin (Fig. 2b), if formed at a temperature of 140°C cured product shows a uniform phase structure similar to the unblended sample. When the formation tem-

perature is raised to 160°C (Fig. 2c) the thermoplastic resin is distributed as isolated globules within a matrix of thermoplastic resin. Higher formation temperatures, raised to 180°C (Fig. 2d), result in a continuous phase formation intermediate between thermosetting and thermoplastic resins. In this way, controlling the phase structure of the cured resin by changing the formation temperature, it is possible to obtain a thermosetting/thermoplastic hybrid in which the thermoplastic resin forms a continuous phase structure.

We subsequently carried out comparative tests of the decomposability of the unblended cured thermosetting resin and a cured thermosetting/thermoplastic hybrid formed with the thermoplastic resin in continuous phase.

DECOMPOSABILITY OF THE CURED HYBRID. We dissolved the thermoplastic resin used in this experiment in DMF (dimethylformamide) and other organic solvents. We then evaluated the decomposability by organic-solvent treatment with DMF of the cured unblended thermoset-

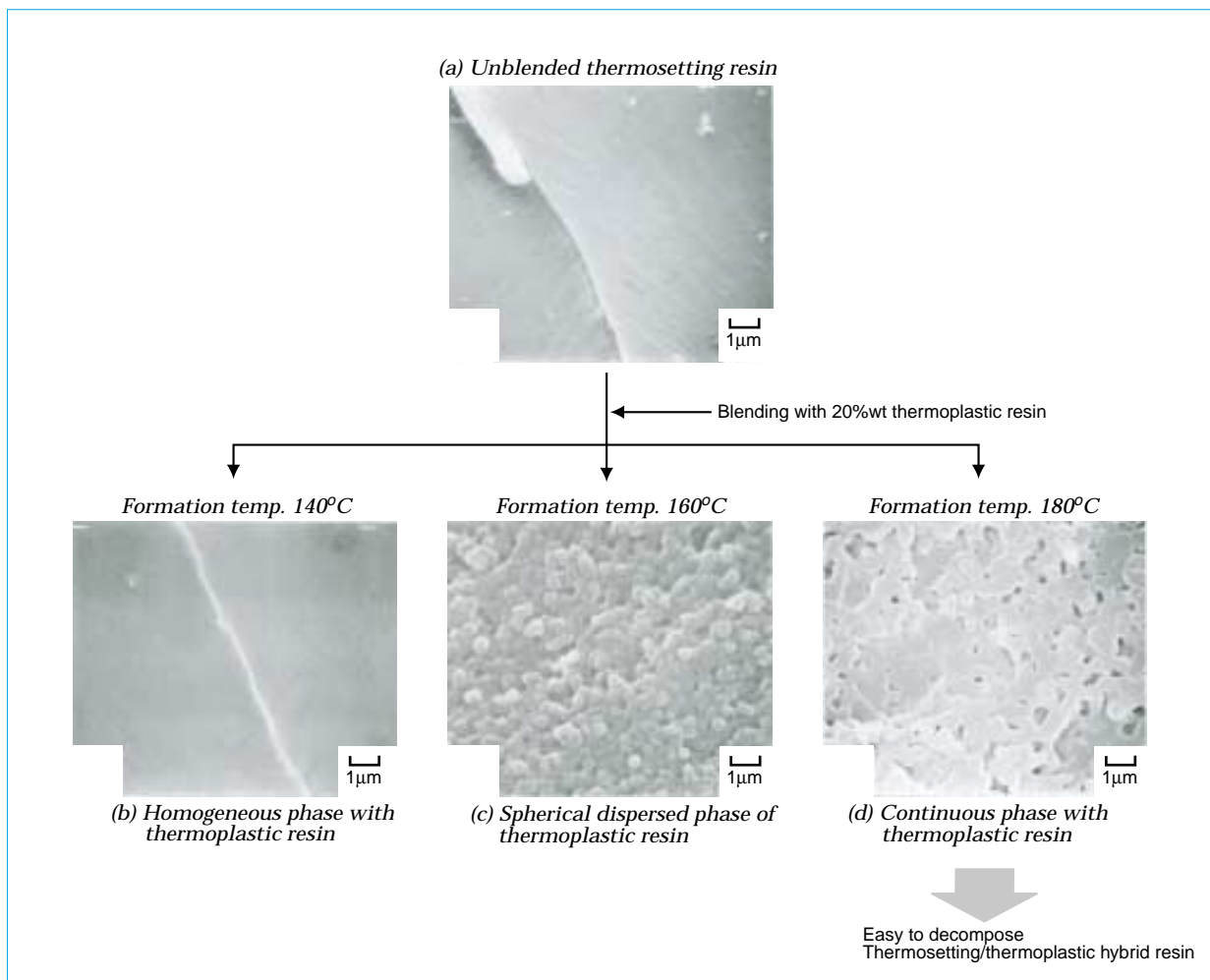


Fig. 2 Scanning electron micrographs of the cured resins.

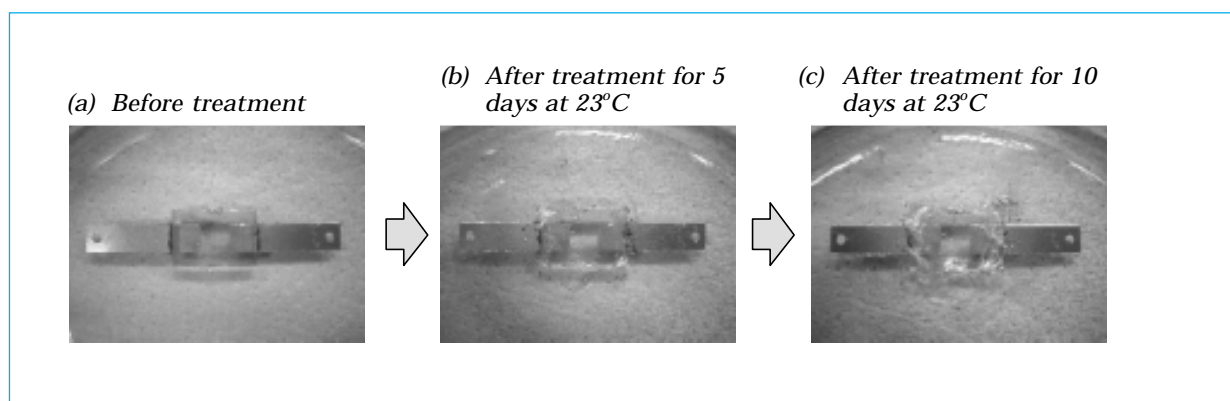


Fig. 3 Organic solvent treatment of cured thermosetting resin

ting resin in comparison with the cured thermosetting/thermoplastic hybrid. We used drawing-out adhesion test pieces for evaluation.

Fig. 3 shows how the adhesion test piece of the cured unblended thermosetting resin changed upon treatment with organic solvent. Even after five days of treatment at room temperature (23°C), the outward appearance of the test piece of the cured unblended thermosetting resin was unchanged (Fig 3b). Although outward alteration of the resin body was observed ten days after the start of treatment, the metal part in the resin body remained firmly embedded (Fig 3c). This demonstrates the processing issues that arise from the insolubility of the cured unblended thermosetting resin.

Fig. 4 shows how the drawing-out adhesion test piece of the cured thermosetting/thermoplastic hybrid was changed by treatment with organic solvent. Fig 4a shows the test piece before the start of treatment. Owing to the phase separation of the included thermoplastic resin, the cured product is not transparent. During organic solvent treatment with DMF of the cured thermosetting/thermoplastic hybrid, surface dissolution of the resin body was observed after a few hours of treatment. After 24 hours,

advanced dissolution of the resin body became quite apparent (Fig. 4b). Then, two days (50 hours) after the start of treatment, the resin body was finely broken down and the embedded metal part could be separated and recovered (Fig. 4c).

PROPERTIES OF THE HYBRID RESIN. Table 1 shows the thermal and mechanical properties of the cured hybrid. It had greater flexural strength than unblended thermosetting resin, while data for both elongation and elasticity indicate similar but higher values. Fracture toughness of the cured hybrid was much higher than for cured thermosetting resin, being almost double (1.9 times higher). As opposed to a heat sensitivity Tg value of 150°C for cured unblended thermosetting resin, the value for the thermosetting/thermoplastic hybrid, at 158°C, was 8°C higher.

As described above, the blending of thermoplastic resin with thermosetting resin is a recognized technique for improving the former's properties. The thermosetting resin that we tested, after this kind of blending with thermoplastic resin, showed improved temperature sensitivity and toughness that gave the cured resin high-temperature sensitivity and strength com-

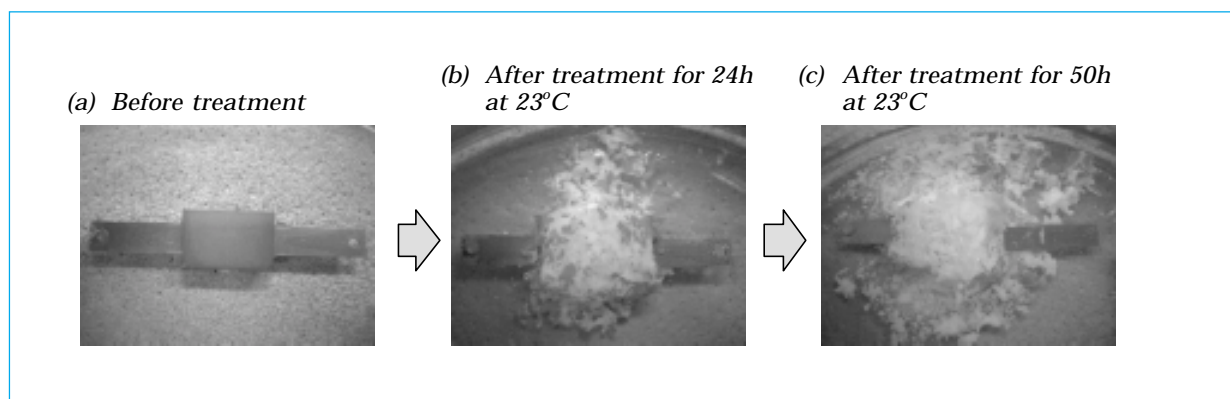


Fig. 4 Organic solvent treatment of cured thermosetting/thermoplastic hybrid

Table 1 Thermal and Mechanical Properties of Cured Resins

Test material	Flexural properties			Fracture toughness value K _c (MN/m ^{3/2})	T _g (DMA) (°C)
	Strength (MPa)	Distortion (%)	Modulus (GPa)		
Unblended thermosetting resin	123±6	6.50±1.54	2.71±0.09	0.83±0.03	151
Thermosetting/thermoplastic hybrid	127±7	7.14±2.83	2.89±0.01	1.55±0.08	159

parable with engineering plastics.

Without the use of high polymer thermoplastic resin, however, any improvement in properties would be slight. Even so, these advantages are offset by poorer handling, which results from the rapid increase in viscosity that accompanies blending. Consequently, the next challenge will be to find a practical technique for reducing viscosity at the time of thermoplastic resin blending.

Evaluations of a hybrid resin formed by blending small amounts of thermoplastic resin with a thermosetting resin show that it possesses important advantages in terms of easy decomposition. This enables metal and other parts with intrinsic value for recycling to be recovered despite being embedded in plastic. It also has improved physical properties. Mitsubishi Electric is now addressing the problem of the high viscosity of the blended resin. □

References

- [1] Mimura K., Ito H., Fujioka H.: Improvement of thermal and mechanical properties by control morphologies in PES-modified epoxy resins, *Polymer* 41, 4451 (2000)
- [2] Mimura K., Ito H.: The characteristics of epoxy resin that makes decomposition easy by blending thermoplastic polymer, *J. of Applied Polymer Science* 89, 527 (2003).

Recovering Phosphates from Sewage Sludge

by Nozomu Yasunaga and Junji Hirotsuji*

To avoid both the impending exhaustion of phosphate resources and the eutrophication of water environments, it is important to develop phosphorous recycling technology. In response, there has been some progress in developing technology to recover phosphates from sewage sludge. By carrying out alkali treatment after injecting ozone into sewage sludge containing phosphates, a synergistic effect enhances the elution of phosphates from the sludge. Experiments have shown that in 15 minutes 80% of the phosphorous is eluted from such sludge.

Background and Objectives

The total global amount of phosphate rock mined annually is 150 million tons and resources will be exhausted in 30 or 40 years if this continues. Japan is almost completely dependent on imports of phosphate rock and thus the impending exhaustion of world stocks is of particular concern.

Even though there is little social awareness of the problem, it is necessary to respond rapidly to the impending crisis. At the same time, the build up of phosphates in Japan has led to conspicuous eutrophication of water environments. To resolve both of these issues, it is important to develop phosphorous recycling technology.

Somewhere between 10% and 20% of the phosphorous in imported phosphate rock ends up in sewage sludge. While processing to remove phosphorous from sewage water as it undergoes treatment is becoming more widespread to counteract eutrophication of water environments, the amount of phosphates in sewage sludge is increasing. It therefore becomes important to recover phosphates from sewage sludge. Working towards the goal of developing a system to effectively recover phosphates, we have been developing a treatment technology that achieves this by rapidly and highly efficiently eluting phosphates from sewage sludge (Fig. 1). In this article we discuss the investigations that led us to this method and consider the mechanics of the phosphate elution.

Experimental Conditions and Method

We examined four treatment methods: heat, ultrasonic homogenization, ozone, and addition of acid or alkali. We investigated the first three methods independently and tested acid and alkali in combination with other treatments. Furthermore, only stirring sewage sludge was tested as a control. For the heat treatment the sewage sludge was raised to a specified temperature (70°C) while stirring it to ensure uniform temperature distribution. The sewage sludge was

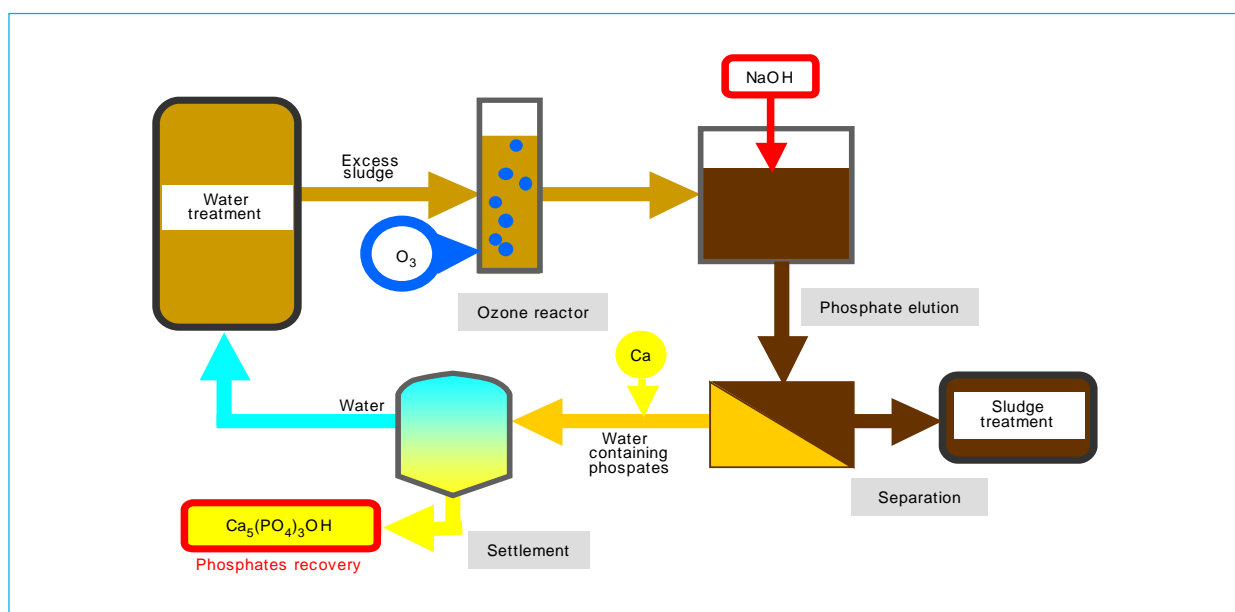


Fig. 1 System to recover phosphates from sewage sludge.

*Nozomu Yasunaga and Junji Hirotsuji are with the Advanced Technology R&D Center.

maintained at this temperature for 30 to 60 minutes. Ultrasonic homogenization (60W, 19.9kHz) was also carried out for 30 to 60 minutes while stirring to ensure uniform homogenization. Injection of ozone was discontinued after one to ten minutes to suppress foaming. After each of these processes, to carry out an acid or alkali treatment, solutions of either 1mol/L of hydrochloric acid or 1mol/L of sodium hydroxide were used to adjust the pH, after which the sludge was stirred for five minutes.

The sludge used in this experiment was obtained from the aeration tank of a sewage treatment plant. It was activated sludge, rendered favorable for the removal of phosphorous; the phosphate concentration in the secondary treated water was less than 1mg/L. In each of the experiments the suspended solid (SS) concentration was adjusted to between 2,000 to 3,000mg/L. All of the activated sludge samples used for each process trial were 450mL samples that had been previously analyzed for total phosphorus (T-P) concentration. After processing, the samples were passed through a 1 μ m pore-size glass filter. The concentrations of soluble phosphate (S-P) and orthophosphate ($\text{PO}_4^{3-}\text{-P}$) remaining in the sample were then measured. The difference in the results for each was taken to be the concentration of poly-P (polyphosphate: phosphate polymer composed of chains of from three to a thousand units of orthophosphate, $[\text{PO}_3]_n$, where $n = 3\text{-}1,000$).

Results and Discussion

Fig. 2 shows phosphate elution results for each of the treatments we tested in combination with alkali processing. In each instance, much more

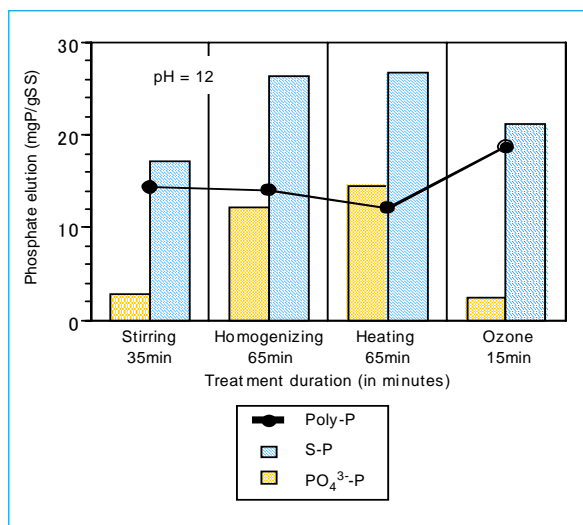


Fig. 2 Changes in phosphate elution when various treatments are combined with alkali treatment

phosphate was eluted after the addition of alkali than by the addition of acid. This finding shows that alkali treatment is effective for phosphate elution. In particular, if alkali is added after ozone processing (which we have called “ozone + alkali treatment” below), polyphosphate can be eluted in a short processing time. Upon discovering this, we decided to investigate ozone + alkali treatment in more detail.

Fig. 3 shows the difference in elution results of treatment solely with alkali or ozone and combined treatment with ozone + alkali. With ozone

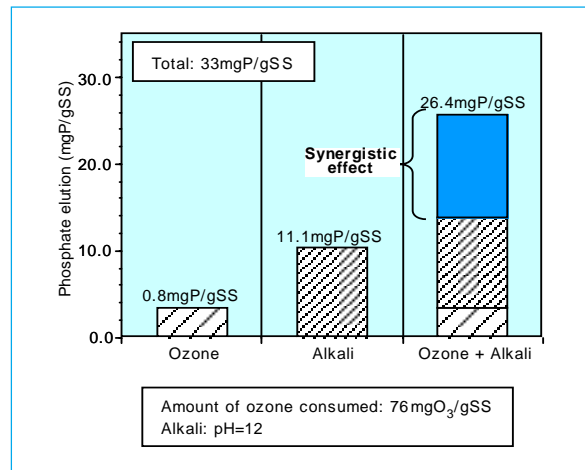


Fig. 3 Amounts of phosphate eluted by ozone + alkali treatment

treatment alone, with a total consumption of 76mg of ozone per gSS, not even as little as 3.4mgP/gSS was eluted. Moreover, using solely alkali treatment, at the pH12 level, only 10.0mgP/gSS was eluted. By contrast, treatment with pH12 level alkali consuming 76mgO₃/gSS of ozone resulted in phosphate elution of 26mgP/gSS, or about 80% of the phosphorus (32mgP/gSS) in the sludge. This was greater than the sum of phosphate elution resulting from treatment solely with alkali and solely with ozone. We therefore understood that a synergistic phosphate elution effect results when alkali is added after ozone injection.

Next, we carried out detailed investigation into the effects of varying the amount of ozone consumed and pH level. Fig. 4 shows the relationship between ozone consumption and phosphate elution. Alkali treatment is exceptionally effective in achieving phosphate elution from sewage sludge. Our findings show that the higher the pH, and the higher the amount of ozone consumed, the greater was the resultant phosphate elution. No synergistic effect was observed when ozone consumption was less than 18mgO₃/gSS. Above that level, the synergistic

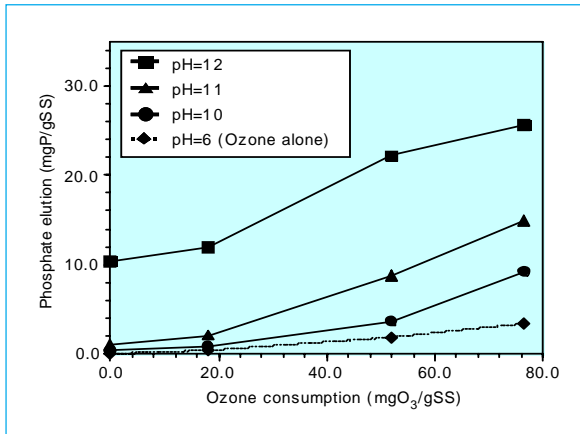


Fig. 4 Amounts of ozone consumed vs. amounts of phosphate eluted for ozone + alkali treatment.

effect increased with increasing amounts of ozone consumption.

To optimize the phosphate elution technique, it is necessary to grasp the relationship between the damaged sites of the microorganism (sludge) and phosphate elution. To do this it is necessary to elucidate the damage mechanism for the microorganisms. Even in research specifically directed at sterilization technology, however, specifying and detailing the damaged site is difficult. We therefore used an indirect method of investigation to reach an understanding of the mechanism of phosphate elution. Knowing that the nucleic acid of microorganisms absorbs light with a wavelength of 260nm, we decided to compare absorption results before and after treatment with alkali or ozone alone, and with ozone + alkali. This would provide evidence of whether the cell contents were eluted and thus enable us to check whether the cell membranes had been breached. Fig. 5 shows the relationship between absorbance and the amount of phosphate elution. These results indicate that it is not only phosphate that is specifically eluted: the endoplasmic content of cells in the filtrate also increases in a fixed ratio as the concentration of phosphate rises. The cell membranes of the sludge were probably broken down by the

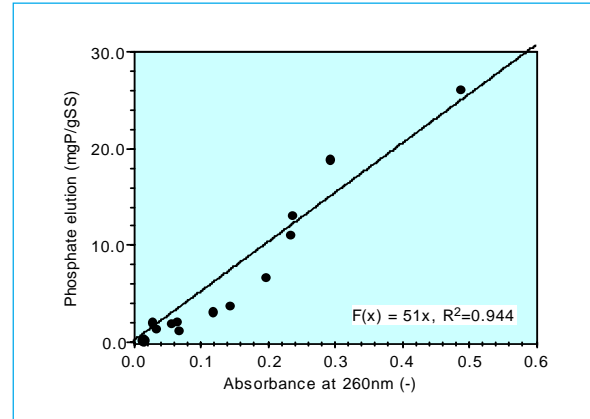


Fig. 5 Absorbance at 260nm vs. amounts of phosphate eluted by ozone + alkali treatment

ozone and many dead microorganisms might be present. However, even after extended treatment with ozone alone, the amount of phosphate in the sludge that was eluted into the liquid phase did not increase. When, after injection of ozone, alkali was added, the amount of phosphate that was eluted from the sludge was greater than the sum of phosphate elution using the ozone and alkali treatments alone. This is probably because the proteins and lipids that make up the cell membranes and cell walls of the sludge react with the ozone, resulting in partial damage to them. Then, when alkali is added, these sites damaged by ozone are dissolved preferentially in reaction to the alkali. We conjecture that this is why such a large amount of phosphate was eluted into the liquid. Fig. 6 illustrates the hypothetical mechanisms involved in the process, discussed above, of phosphate elution from sewage sludge using the ozone + alkali treatment.

Conclusions

We investigated how to develop a way of eluting phosphates that would be both fast and efficient. This article reports the trials of the resulting method.

Firstly, ozone + alkali treatment is effective

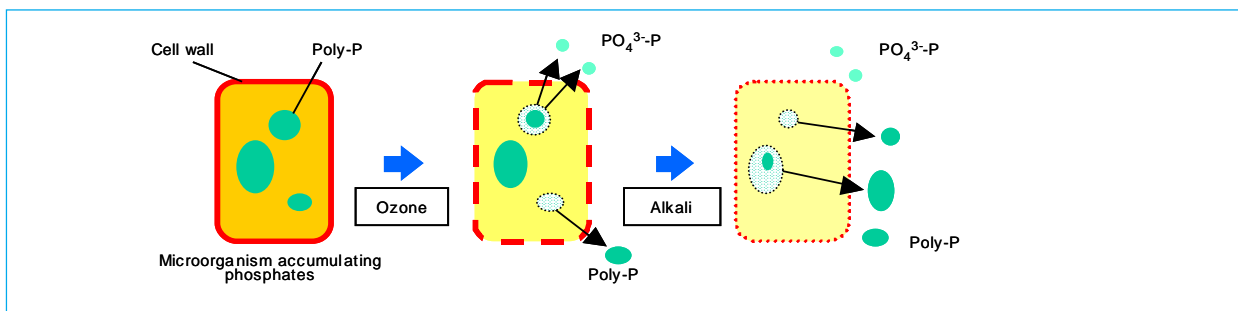


Fig. 6 Hypothetical mechanism of phosphate elution from microorganisms by ozone + alkali treatment

for phosphate elution. That is, injection of ozone into sludge followed by the addition of alkali is a rapid and highly efficient method of achieving phosphate elution. Secondly, a synergistic effect on phosphate elution is obtained from the ozone + alkali treatment: during treatment for 15 minutes, 80% of the phosphate is eluted from the sludge. Finally, we conjecture that the mechanisms causing this enhanced phosphate elution are as follows. Ozone causes partial damage to the cell walls and cell membranes due to the reaction of ozone with their proteins and lipids. This partial damage promotes the dissolution of the cell walls and cell membranes by the alkali. These mechanisms would account for the elution of large amounts of endoplasmic matter in the liquid along with large amounts of phosphate.

We will continue to examine the optimal conditions for phosphate elution and investigate means of recovering the eluted phosphate. □

This work was supported by the New Energy and Industrial Technology Development Organization (NEDO). The authors wish to thank the members of NEDO.

Clean Combustion for Use in Indoor Environments

by Minoru Sato and Hiroaki Shigeoka*

To achieve a more compact open-type space heater, the burner structure has been changed to bring the supply of secondary combustion air into proximity with the primary flame. While ensuring both the prevention of carbon monoxide (CO) emissions and a shorter secondary flame, we succeeded in reducing the size of the combustion chamber to one third. Furthermore, the use of catalytically assisted combustion technology has enabled clean combustion with NO_x (nitrogen oxide) emission values reduced to half the permissible level.

The Space-Heater Market in Japan

In Japan, the market for combustion-type space heaters for home use divides mainly into closed and open types. Formerly, forced-draft directly vented heaters were common. Recently, fan heaters have become more popular: their easy set up is making them the mainstream heaters for Japanese homes. In forced-draft direct-vent heaters, the combustion circuit is isolated from the room space and the flue gas is vented to the outside air after passing through heat exchangers that heat the room space. In fan heaters, the combustion circuit is open to the room and the spent flue gas passes directly into the room space. If they are not to foul indoor air, open-type space heaters must therefore burn fuel cleanly.

Special attention must be paid to the emission of carbon monoxide and NO_x by open-type space heaters. Carbon monoxide gas emissions result from the incomplete combustion of hydrocarbon fuels. Because of the serious risk to human life, carbon monoxide emissions must conform with JIS (Japanese Industrial Standards) regulations. Since 1990, when NO_x was first regulated by the JGKA (Japan Industrial Association of Kerosene and Gas Appliances), NO_x emissions have been subject to increasingly strict control every year.

Compact Combustion

Fig. 1 shows the structure of a fan-assisted oil heater. The hot flue gas is mixed with a large volume of indoor air by a circulating fan and, at a suitable temperature, expelled from the fan heater to supply heat to the room. The combustion method involves the burning of premixed kerosene vapor and air in the burner. For primary air, the theoretical volume of air in the premixture is supplied with an air ratio of about 0.8:1. Fuel-rich primary flames are formed at several dozen sites on the burner. A convection fan at the rear of the combustion chamber supplies the remaining air (secondary air) that is required to complete combustion. The combustion reaction is carried to completion by the formation of a secondary flame. Because the secondary flame burns in a less intense reaction and at a lower temperature than the primary flame, it is necessary to increase the size of the combustion chamber to accommodate it.

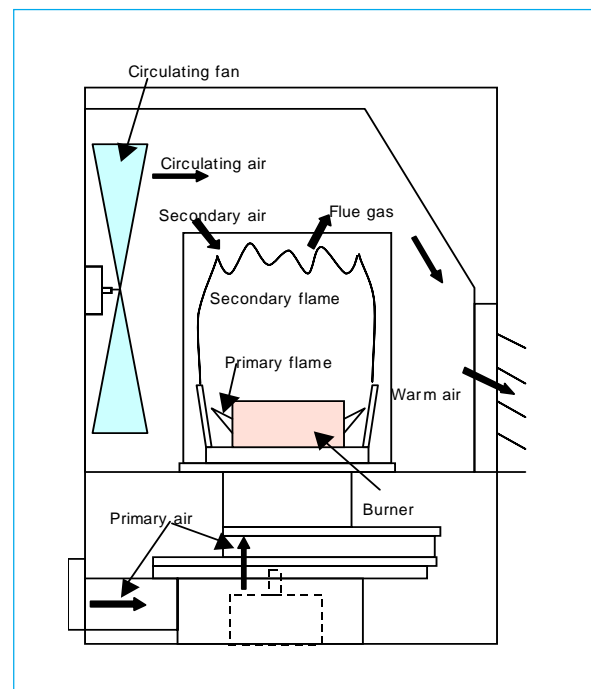


Fig. 1 Structure of a fan-assisted oil heater

To decrease the size of the secondary flame we changed the air-supply method and burner structure as shown in Figs. 2 and 3. In the modified burner, the secondary air supply passes both through the center of the burner and around the burner so that it converges over the primary flame. The size of the secondary flame is thus greatly reduced. This structure enabled us to reduce the 3.5 liter volume of the combustion chamber that was needed in previous designs to 1.1 liter, a form factor reduction to about one third.

*Minoru Sato and Hiroaki Shigeoka are with the Advanced Technology R&D Center.

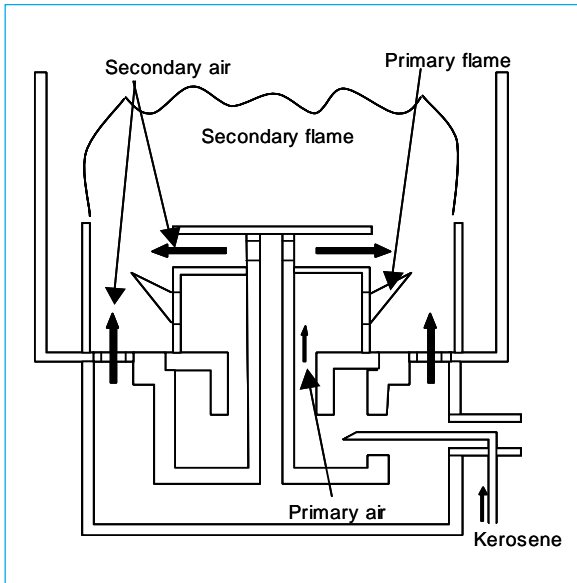


Fig. 2 Structure of the compact burner

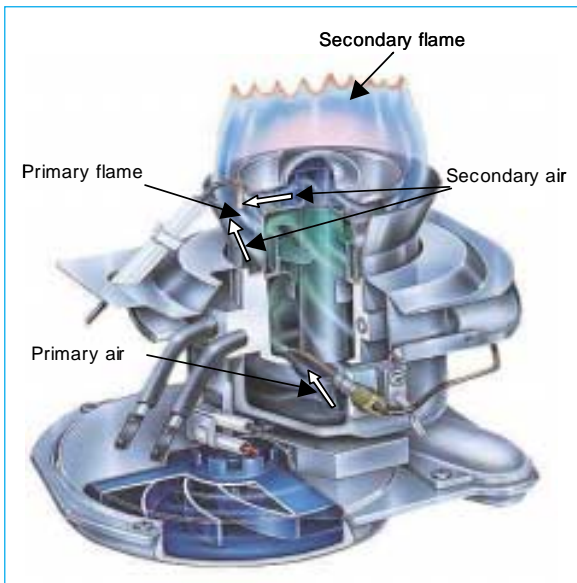


Fig. 3 Cutaway illustration of the compact burner.

The combustion rate for household heaters is adjusted as necessary. It is highly desirable to extend the range of combustion rates supported by the burner, from high to lower, because this determines the volume of room space that can be heated, the amount of insulation required, etc. Currently, most of the combustion heaters sold in Japan have a high rate of combustion in the range of 3.0 to 3.5kW. The burner largely determines weak combustion performance. With the burner that is shown in Fig. 2, in which the secondary air effectively suppresses carbon monoxide emissions, it is possible to considerably extend the range of weak combustion. From a previous five-fold adjustment range of 3.2kW to 0.63kW, the new design extends it to seven fold, from 3.5kW down to 0.5kW.

If dust accumulation reduces the amount of air available for combustion, or the amount of oxygen in the room is reduced by poor room ventilation, and in certain other circumstances, carbon monoxide may be generated by a fan heater. It is essential to equip a fan heater with sensors that can detect such incomplete combustion as soon as possible and trigger automatic heater shut down. To detect the state of combustion in oil-burning fan heaters, the flame ion-current method is used. When an electric field is applied to the flame, an electric current of the order of a few microamps flows that is highly dependent on the state of combustion. When the flame emits excess carbon monoxide, the flame ion current decreases. If the flame ion current falls below the preset lower limit that will still prevent incomplete combustion, the control sequence to turn off the heater is initiated.

Catalytically Assisted Combustion

Catalytic combustion is a technique that generates thermal energy while carrying out the oxidation reaction of fuel and air in the presence of a catalyst. During catalytic combustion, all the supplied fuel is normally reacted in the presence of the catalyst. This method imposes a high combustion load per unit volume of catalyst, heating it to such high temperatures that it tends to deteriorate. One way around this problem is to use a catalytically assisted combustion method to reduce the operating temperature of the catalyst. As shown in Fig. 4, only part of the fuel is reacted in the presence of the catalyst and the remaining non-reacted fuel vapor, as it passes out of the reactor in parallel with reacted gas, undergoes a gas-phase reaction (flame combustion). In this method, the hot, catalytically reacted flue gas has a stabilizing effect on the gas phase and it is possible to use a leaner fuel-air mixture for combustion. The leaner mixture enables the flame combustion to take place at a lower temperature and this reduces the amount of NOx emissions.

The type of catalytically assisted combustion that we investigated has a number of features. First of all, catalytic and non-catalytic channels are arranged adjacently in parallel. Consequently, the fuel-air mixture that passes through the non-catalytic channels is not reacted and performs the role of cooling the reactor channels. When the non-reacted fuel-air mixture emerges from the non-catalytic channels it undergoes gas-phase reaction. In addition, the rectangular form of the catalytic channels increases the surface available for heat generation.

Fig. 5 presents test data indicating how the amount of air in the fuel-air mixture affects the

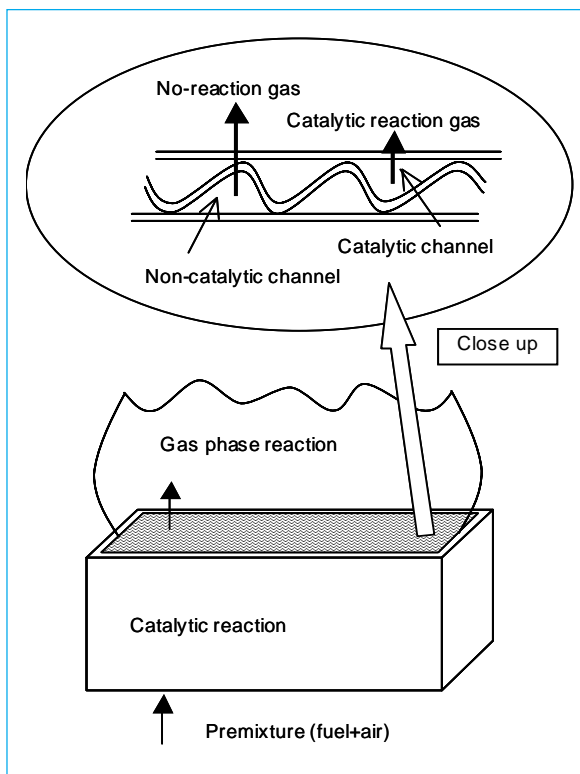


Fig. 4 Catalytically assisted combustion

exhaust-gas characteristics (CO, NO_x) and catalyst temperature. At lower air ratios of 1.2 to 1.4:1, the gas-phase reaction takes place right on top of the catalytic reactor as soon as the non-reacted mixture emerges. Under these con-

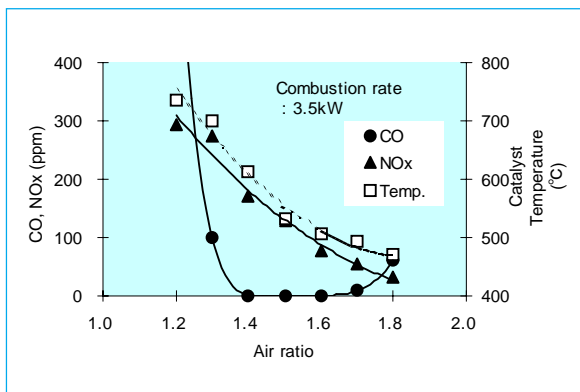


Fig. 5 Emission characteristics of catalytically assisted combustion

ditions the gas-phase reaction occurs at a high temperature and NO_x emissions are comparatively high at 150 to 300ppm. Increasing the air ratio results in the gas-phase reaction occurring further along the stream flow. When the air ratio is raised to 1.6:1, the gas-phase reaction lifts off the reactor exits. NO_x emissions decrease with increasing air ratio: at an air ratio of 1.7:1 NO_x is cut to 50ppm. At this point, the catalyst temperature, at around 500°C, is above the activation temperature. Accordingly, we observed

that the gas-phase reaction that occurs later in the flow was stabilized by the portion of fuel-air mixture that had been raised to high temperature due to the catalytic oxidation. At this air ratio, the level of carbon monoxide emissions was also low. Since the gas-phase reaction ended about 120mm beyond the exits of the catalytic reactor, it was possible to contain the burner within a compact combustion chamber.

Fig. 6 shows the air-ratio conditions when the

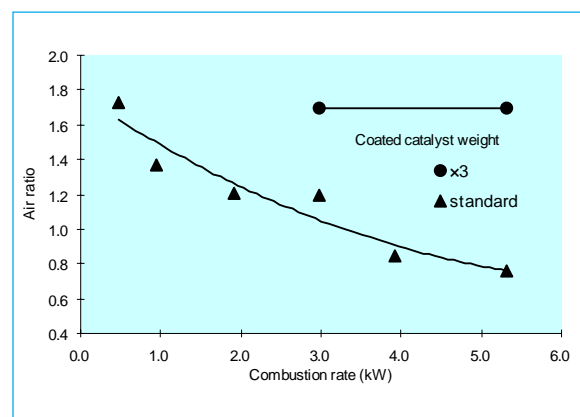


Fig. 6 The heat-resistance limits of catalyst thickness

catalyst temperature is 900°C. At air-ratio ranges lower than those shown, the catalyst temperature exceeds 900°C. In view of the actual ability of the catalyst to withstand heat, these values represent the lower limits of the air ratio. At a high combustion rate and in the lower ranges of air ratios, combustion equivalent to 5.3kW is possible with an air ratio of 0.8:1. For lower combustion rates, the speed of the flow of fuel-air mixture through the reactor is reduced. This results in higher catalyst temperatures. At 0.5kW, the lower air-ratio limit must be 1.7:1.

We also investigated the effect of catalyst coating weight. A threefold increase in the weight of the coating increased the amount of heat generated by the catalytic reaction, as shown by the straight horizontal line in Fig. 6. At a combustion rate of 5.3kW, increasing the air ratio to 1.7:1 raises the catalyst temperature to 900°C. Although a weightier coating of catalyst is advantageous for increased durability, it also tends to restrict the range of usable heating capacities. It is therefore important to select the optimal weight of coating according to design conditions.

The article shows how we confirmed that catalytically assisted combustion both reduces NO_x emissions and effectively reduces the catalyst operating temperature. Even so, to make the system practical we still need to carry out further investigations into combustion detection methods and to deal with cost-reduction issues. □

Plasma PFC Abatement at Atmospheric Pressure

by Yasutaka Inanaga and Kiyohiko Yoshida*

The PFCs (perfluoro compounds) that are used in semiconductor fabrication processes have an extremely high global warming potential (GWP). This is why reduction in the amount of their emissions by 2010 have been subject to international agreement.^{[1],[2]} We have established a highly efficient method of decomposing PFCs under atmospheric pressure with microwave-induced plasma. Here we present an outline of the equipment and some abatement performance results.

The Equipment Used

Fig. 1 shows the process flow of PFC abatement using microwave-induced plasma under atmospheric pressure. Microwave discharge enables the generation of stable plasma with modest levels of electrical power consumption. The high

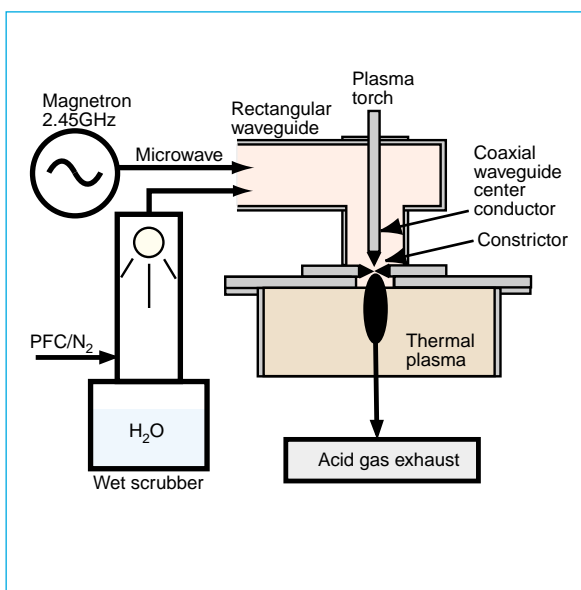


Fig. 1 Process flow of PFC abatement system using microwave induced plasma under atmospheric pressure.

temperature of the plasma makes it extremely effective for decomposing harmful gases.

The system uses a 2.45GHz magnetron as the microwave source. After a rectangular waveguide transmits the microwaves into a coaxial waveguide, an electrical field is concentrated in the constrictor, where thermal plasma is generated. The center of the coaxial waveguide is moved up and down to match the impedance. To protect the waveguide from corrosive gases and particles contained in the flow vented from semiconductor fabrication tools, a wet scrubber is located upstream of the plasma process. This also serves to supply the water needed for decomposition reactions, for example, of CF_4 , as shown in Formula 1.



To evaluate the destruction removal efficiency (DRE), we carried out decomposition trials on a mixture of CF_4 , the PFC that is most difficult to decompose, and C_2F_6 , the gas typically used for cleaning chemical vapor deposition (CVD) reaction chambers. Mixed with nitrogen, these PFC gases were supplied from gas cylinders.

We used a Fourier-transform infrared (FTIR) spectroscope (Midac IGA-2000; cell length 10mm) to measure the concentrations of PFCs and other by-products. PFC DRE was quantified by measuring the PFC concentration downstream of the abatement equipment with and without plasma.

Furthermore, because the types of reaction with water exemplified by Formula 1 could influence the PFC DRE, the amount of water introduced was measured using a dew-point hygrometer (Panamatrix, CMX-1; measurement range -20°C to 60°C) and adjusted to more than twice the PFC concentration.

Evaluation of PFC Abatement Characteristics

Fig. 2 shows the decomposition results for a total flow rate of 30slm with CF_4 concentrations of 0.67% and 1% (200sccm, 300sccm). When 2.5kW of microwave power was applied, the DRE exceeded 95%. Effective decomposition at low energy cost (84W per slm of the total gas flow rate) was achieved. In the low concentration range of around 1% CF_4 , increasing the amount of PFCs required no increase in the decomposition energy; the same decomposition rate was maintained with the same amount of energy input. However, when the flow rate was increased to above 30slm, the DRE decreased with the amount of nitrogen. Even so, at processing rates above 30slm, when the microwave energy was increased in step with the increasing flow,

*Yasutaka Inanaga is with the Advanced Technology R&D Center and Kiyohiko Yoshida is with the Communication Systems Center.

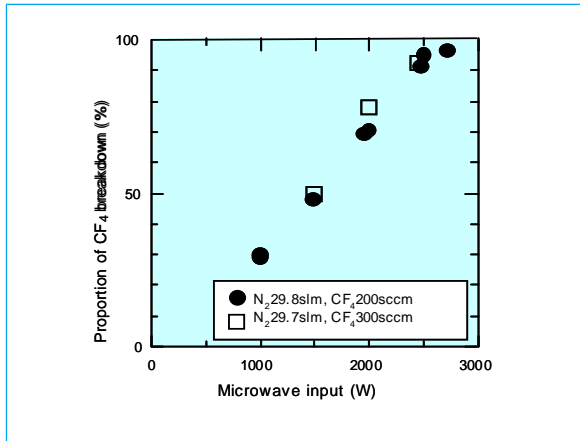


Fig. 2 DRE using microwave induced plasma under atmospheric pressure: CF_4 .

we confirmed that more than 95% decomposition was still possible.

Fig. 3 shows the decomposition characteristics for C_2F_6 . At a diluted flow rate of 150slm, more than 95% DRE at 1% C_2F_6 was achieved with 7.5kW microwave input power. The decomposition of C_2F_6 was lower than that of CF_4 , as with burning or electric-furnace abatement methods.^[5] We found that with our plasma

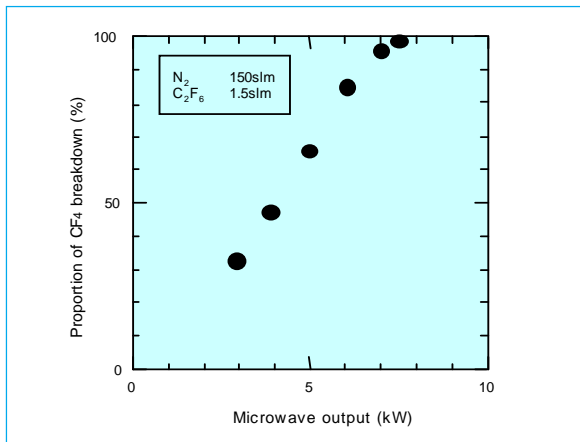


Fig. 3 DRE using microwave induced plasma under atmospheric pressure: C_2F_6 .

method, the energy required for C_2F_6 was 47W/slm, or about half that required for CF_4 . Moreover, from the conditions necessary to achieve DRE exceeding 95% for C_2F_6 , we confirmed that the level of CF_4 generated remained less than 100ppm. This performance is adequate for abatement of global warming.

PFC Abatement System for RIE Processes

Fig. 4 shows the appearance of the PFC abatement system that we developed for reactive ion etching (RIE) processes. Table 1 presents a summary of the specifications. The design is intended to take gas vented from two RIE

chambers and can achieve better than 95% DRE at a flow rate of 30slm (CF_4/N_2). The maximum output of the magnetron is 3kW. Allowing for an aggregate efficiency of 60% for magnetron oscillation and high-voltage power supply, the total power consumption is 5kW.

The gas pipes and waveguides within the abatement equipment have to be proof against corrosive byproducts of the RIE process and PFC decomposition. This is achieved by using resin coatings and anticorrosive metal linings.

One of the advantages of the plasma method is that, unlike combustion methods, it does not



Fig. 4 PFC abatement equipment for RIE tools.

Table 1 Summary Specifications of the Engineering Model

Equipment dimensions	985 x 535 x 1380mm
Equipment weight	250kg (max)
Power consumption	5kW (max)
Nominal flow capacity (of which PFCs)	30slm (200sccm)
PFC DRE	At least 95% (CF_4)
Microwave output	3kW (max)

require fuel. This lowers running costs. Quick startup is another major advantage: the rise in temperature necessary for the decomposition reaction to take place in the process gas occurs the instant the plasma is generated. Utilizing these characteristics of the abatement equipment, it is possible to make the system respond to external signals controlling the microwave

power. This makes it possible to match the microwave power to the status of the RIE process, which would save energy and reduce operational running costs.

To deal with the PFC vented from semiconductor fabrication equipment, we have developed the industry's first abatement system that uses thermal plasma from microwave discharge under atmospheric pressure. It is possible to achieve highly efficient decomposition of 1% CF_4 in the total flow at 83W/slm and C_2F_6 at 47W/slm. □

References

- [1] Kyoto Protocol. Climate Change Conference, Kyoto, Japan. 1997.
- [2] Position Paper Regarding PFC Emission Reduction Goal. World Semiconductor Council, Third Meeting, Fuggi, Italy. 1999.
- [3] Beu, L. et al. Current State of Technology: Perfluorocompound (PFC) Emissions Reduction. International SEMATECH, Technology Transfer #98053508A-TR. 1998.
- [4] Inanaga, Y. et al. Perfluorocompound Decomposition by Plasma under Atmospheric Pressure (in Japanese). Collected Conference Papers, Seidenki Gakkai, 02, 29aB-4, 79-82. 2002.
- [5] Kashihara, M. et al (eds). Systems for Gas Vented during Semiconductor Fabrication and measures to Ensure Safety (in Japanese). pp. 107-122, REALIZE Jigyou Bumon, SIPEC Corporation. 2001.

